Electronic Supplementary Information

Oxygen-vacancy engineered Fe_2O_3 nanoarrays as free-standing electrode for flexible asymmetric supercapacitors

Fenfen Han, Jia Xu, Jie Zhou, Jian Tang* and Weihua Tang*

School of Chemical Engineering, Nanjing University of Science and Technology, Nanjing 210094, P. R. China
E-mail: fnzhoujie@njust.edu.cn and whtang@njust.edu.cn

Table of content

1. Materials characterizations

Morphologies and element distribution of composites were evaluated at field emission scanning electron microscope (FE-SEM, J Hitachi S-4800 at an accelerating voltage of 10 kV). The transmission electron microscope (TEM) images were obtained from FEI Tecnai-12 at an accelerating voltage of 120 kV. High-resolution transmission electron microscopy (HR-TEM) was performed on a FEI Tecnai F30 at an accelerating voltage of 80 kV. X-ray diffraction (XRD) patterns were recorded from Bruker D8 Advance Diffractometer, using the Cu Kα radiation (1.54 Å) at 40 kV and 30 mA. X-ray photoelectron spectroscopy (XPS) analysis were carried out on a Thermo ESCALAB 250 X-ray photoelectron spectrometer with Al Kα radiation (1486.7 eV). Raman spectroscopy (RM 2000 microscopic confocal Raman spectrometer) was performed by employing a 514 nm laser beam. Electron paramagnetic resonance (EPR) spectra were collected from Bruker EMX-10/12.

2. Electrochemical measurements

All electrochemical measurements were carried out on a CHI 760D electrochemical workstation (Shanghai, China). The three-electrode tests were performed in 2 M LiOH solution with a platinum foil as the counter electrode and a saturated calomel electrode as the reference electrode. The conductive memebranes (1.0 cm × 2.0 cm) were used directly as working electrodes. For symmeterical supercapacitor, PVA/LiOH gel was used as solid electrolyte. The areal capacitance in threee-electrode cell is calculated according **Equation S1:**

$$C_A = \frac{I \times \Delta t}{S \times \Delta V} \tag{1}$$

where, I is the discharge current, Δt is the discharged time, S is the electrode area and ΔV is the voltage window.

The areal energy density (E) and power density (P) of symmeterical supercapacitor are calculated according to **Equation S2&3:**

$$E = \frac{1}{2} \times C_A \times \Delta V^2 \tag{2}$$

$$P = \frac{E}{\Delta t} \qquad (3)$$

where, C_A is the areal specific capacitance, Δt is the discharged time, and ΔV is the voltage window.

3. Results and discussions

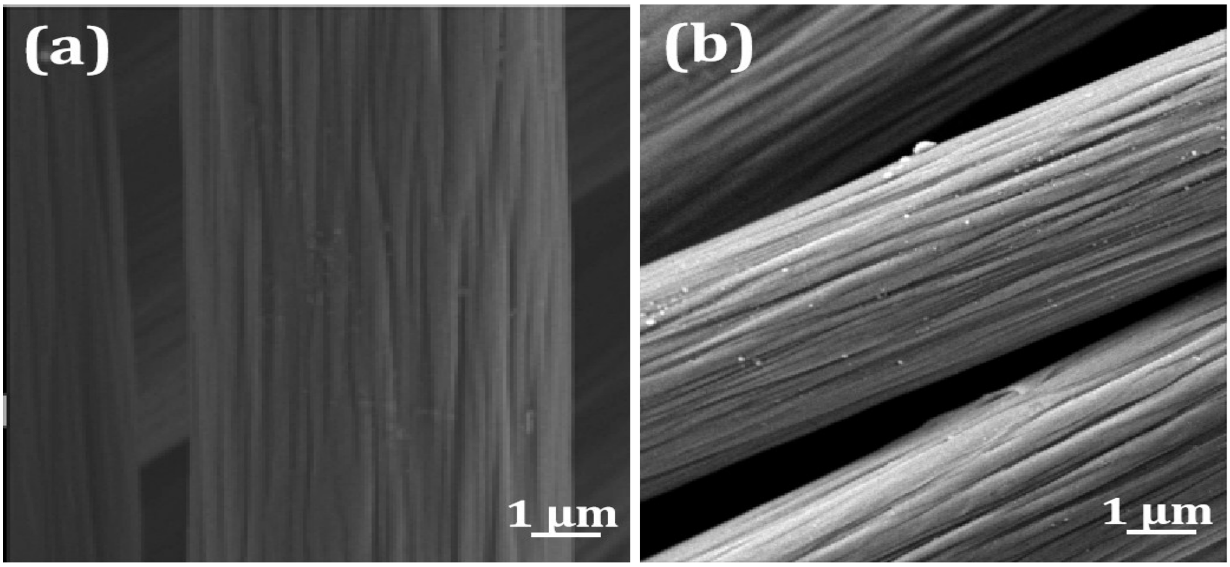

Fig. S1. SEM patterns of (a) pristine CC and PDA coated CC.

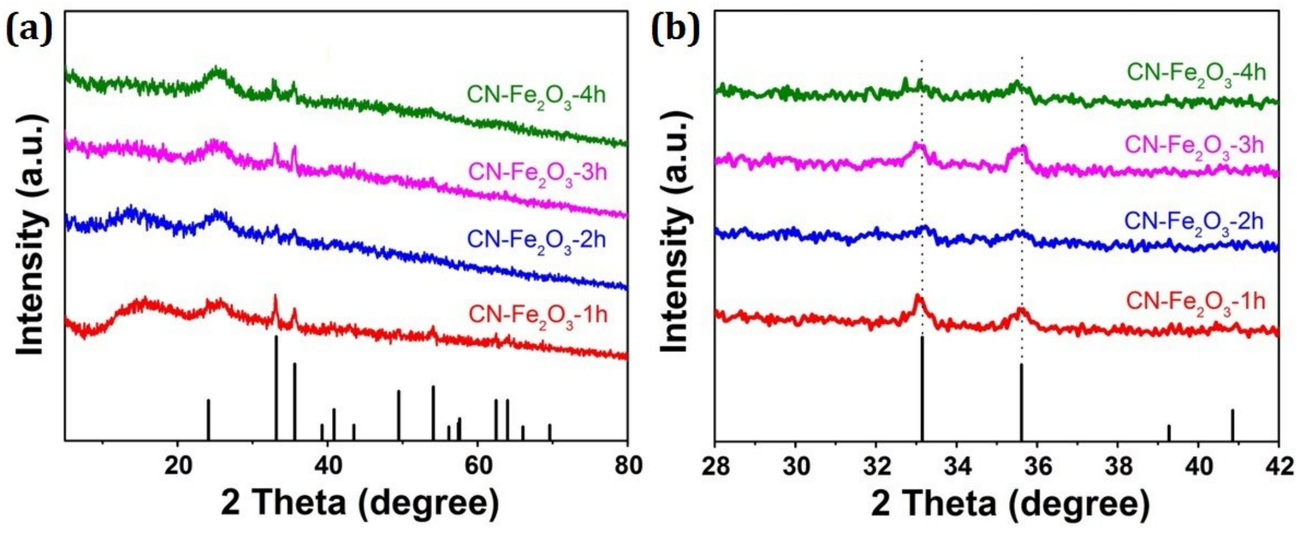

Fig. S2. XRD patterns for CN-Fe_2O_3-1h, CN-Fe_2O_3-2h, CN-Fe_2O_3-3h and CN-Fe_2O_3-4h.

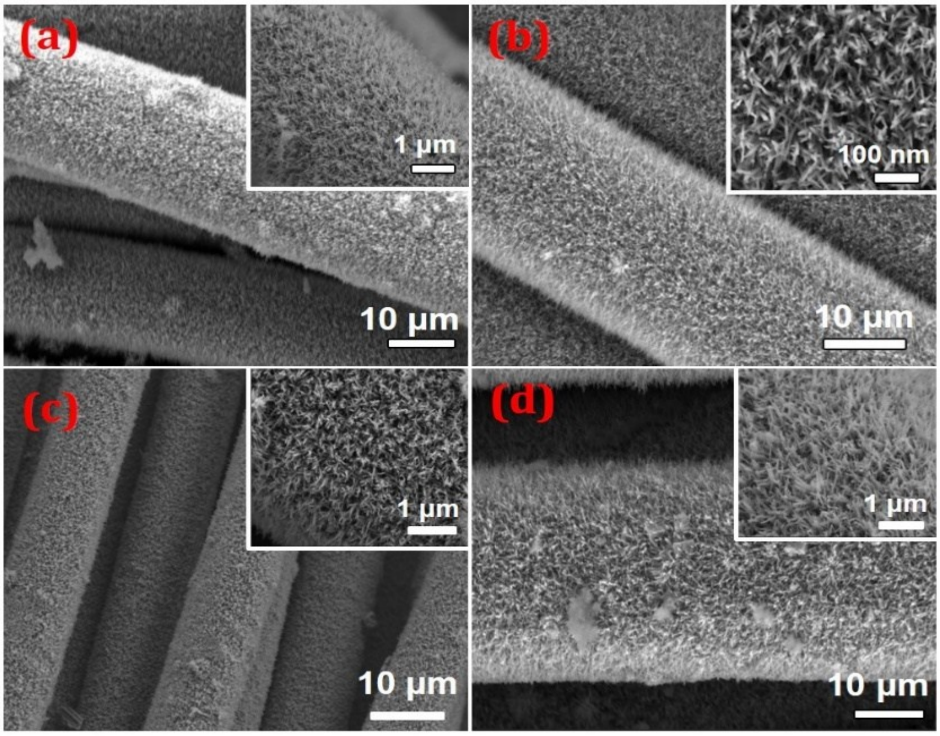

Fig. S3. SEM images for CN-Fe_2O_3 at different reduction time. a) 1 h, b) 2 h, c) 3 h and d) 4 h.

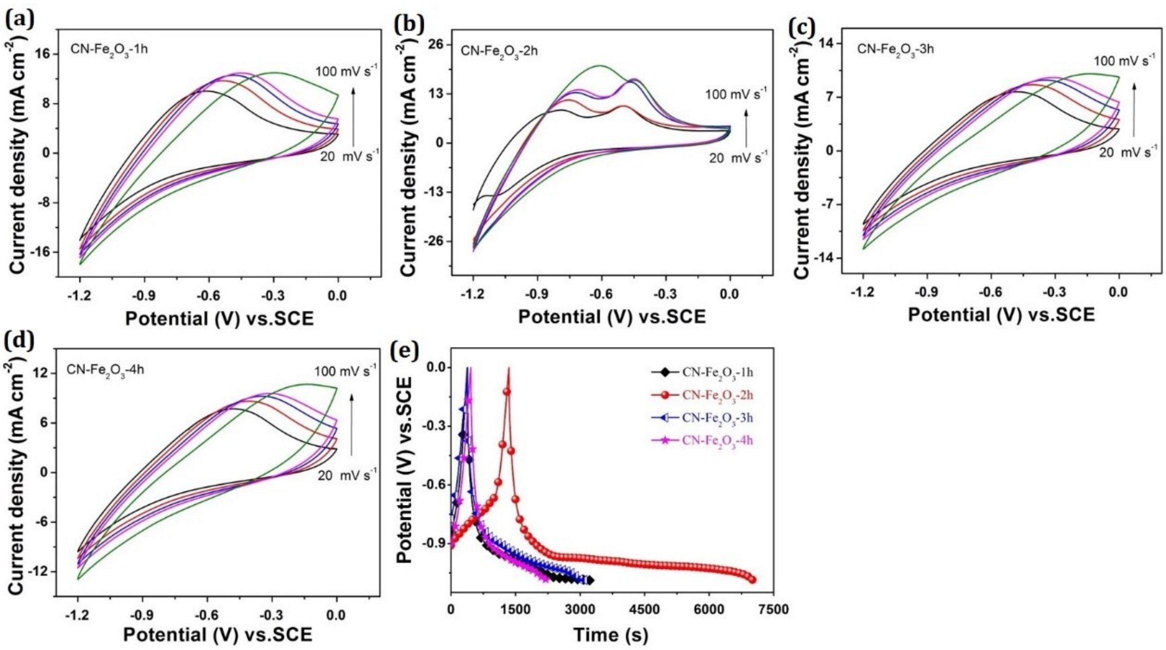

Fig. S4. a-d) CV curves of CN-Fe_2O_3-xh. e) GCD curves of CN-Fe_2O_3-xh at the current density of 0.5 mA cm^{-2}.

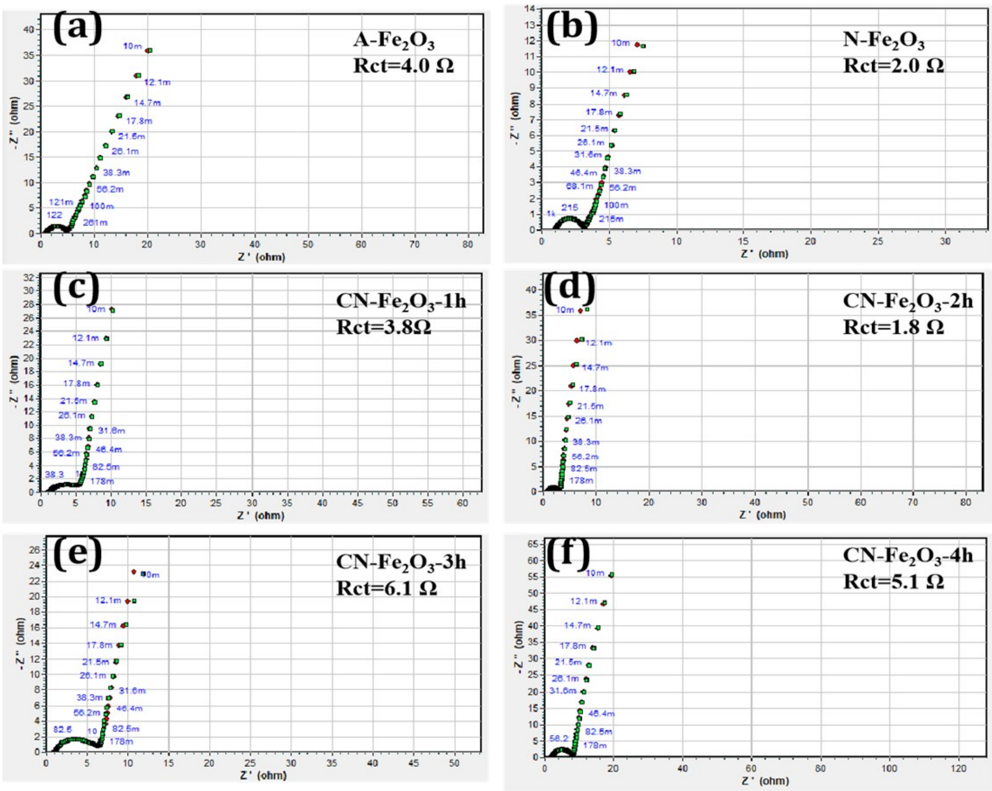

Fig. S5. The fitted Nyquist plots of a) A-Fe_2O_3; b) N-Fe_2O_3; c-d) CN-Fe_2O_3-xh

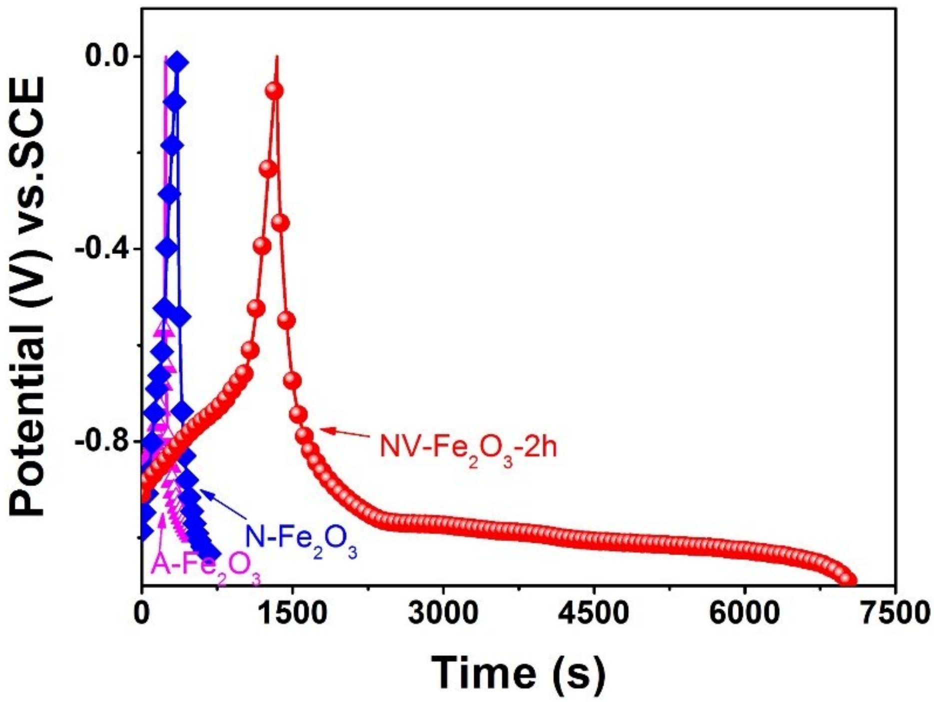

Fig. S6. GCD curves of A-Fe_2O_3, N-Fe_2O_3 and CN-Fe_2O_3-2h at a current density of 0.5 mA cm^{-2}.

Table S1. Comparison of the charge storage with free-standing Fe_2O_3 electrodes.

Electrodes	Voltage window (V)	C_A (F cm^{-2})	Long-term C_A retention	Ref.
ASV-FO	-0.9	0.42 *(0.5 mA cm^{-2})*	90% 5000	S2
N-Fe_2O_3	-0.8	0.38 *(0.5 mA cm^{-2})*	95.2% 10000	S3
SiC@Fe_2O_3	-1.2	1.00 *(0.5 mA cm^{-2})*	86.6% 5000	S4
Fe_2O_3@ACC	-0.8	2.78 *(0.5 mA cm^{-2})*	92% 10000	S5
Fe_2O_3 -P	-0.8	0.34 *(1 mA cm^{-2})*	88% 9000	S6
Ni/GF/H-Fe_2O_3	-1	0.69 *(1 mA cm^{-2})*	95.4% 50000	S7
α-Fe_2O_3/C	-1	0.43 *(1 mA cm^{-2})*	73.2% 4000	S8
S-α-Fe_2O_3@C/OCNTF	-1	1.23 *(2 mA cm^{-2})*	--	S9
CN-Fe_2O_3-2h	-1.1	2.63 *(0.5 mA cm^{-2})*	86.7% 10000	**This work**

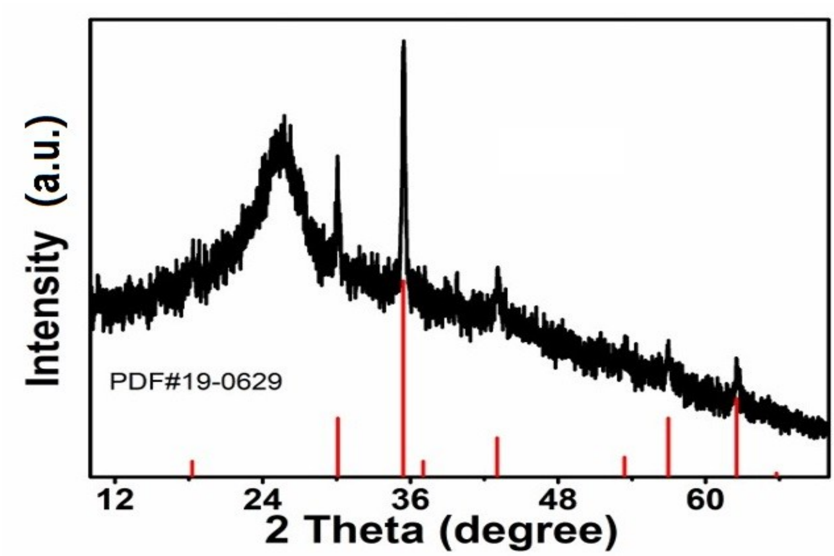

Fig. S7. XRD patterns of CN-Fe_2O_3-2h after long-term cycles.

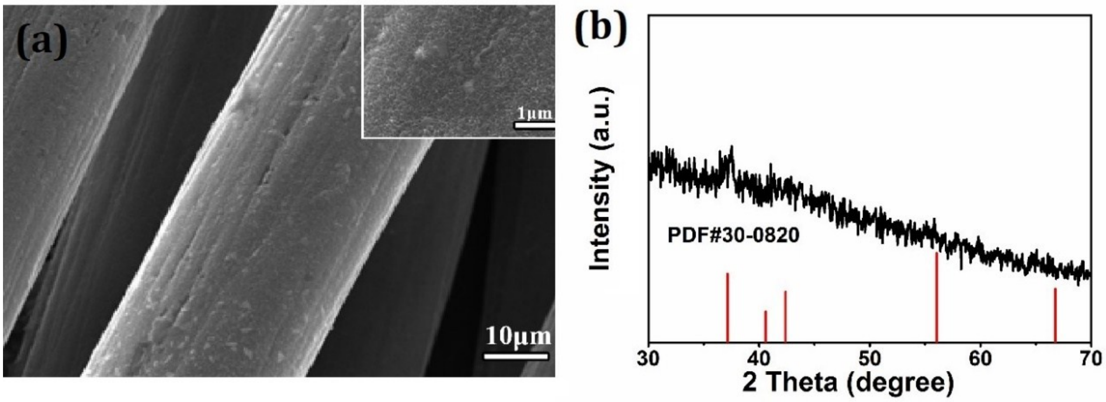

Fig. S8. a) SEM images of MnO_2 on CC fibers. b) XRD patterns of pristine MnO_2.

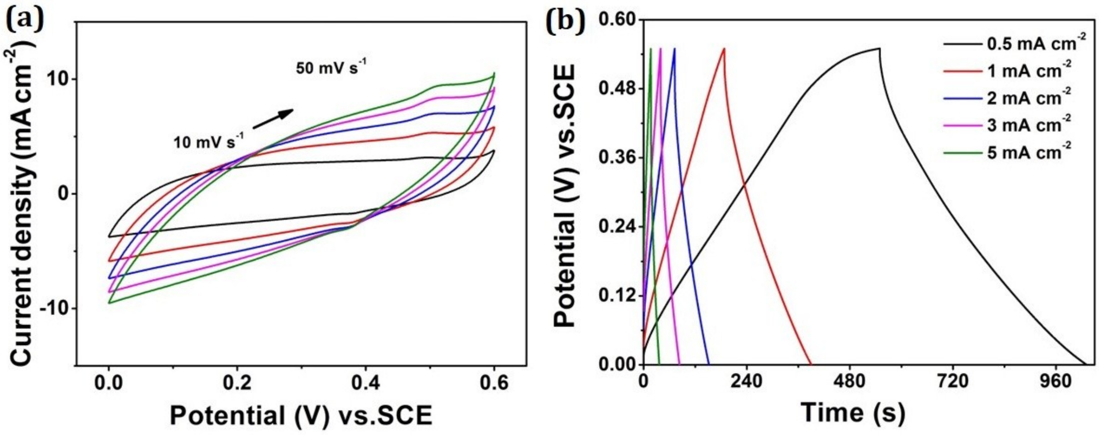

Fig. S9. a) CV curves of MnO_2. b) GCD curves of MnO_2 at different current density from 0.5 mA cm^{-2} to 5 mA cm^{-2}.

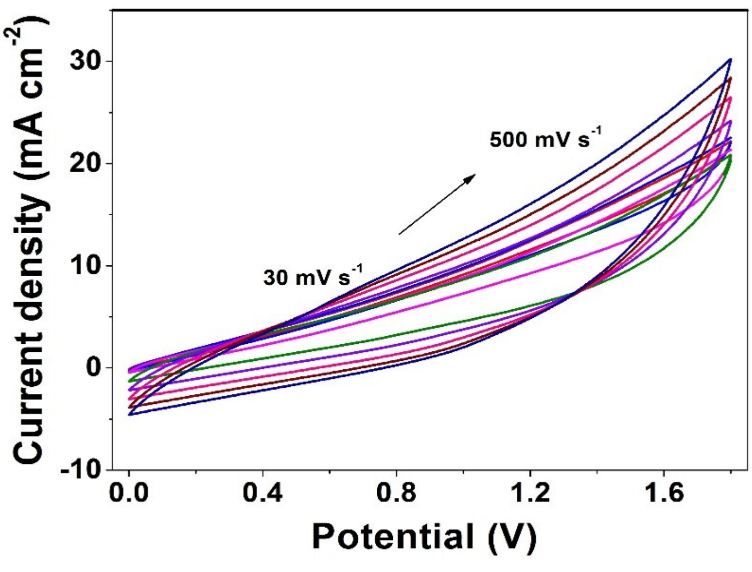

Fig. S10. CV curves of CN-Fe_2O_3-2h//MnO_2 ASC device.

4. References

[S1] Y. Zeng, Y. Han, Y. Zhao, Y. Zeng, M. Yu, Y. Liu, H. Tang, Y. Tong, X. Lu, *Adv. Energy Mater.* 2015, **5**, 1402176.

[S2] S. Sun, T. Zhai, C. Liang, S.V. Savilov and H. Xia, *Nano Energy.* 2018, **45**, 390-397.

[S3] X. Lu, Y. Zeng, M. Yu, T. Zhai, C. Liang, S. Xie, M.S. Balogun and Y. Tong, *Adv. Mater.* 2014, **26**, 3148-3155.

[S4] J. Zhao, Z. Li, X. Yuan, Z. Yang, M. Zhang, A. Meng and Q. Li, *Adv. Energy Mater.* 2018, **8**, 1702787.

[S5] J. Li, Y. Wang, W. Xu, Y. Wang, B. Zhang, S. Luo, X. Zhou, C. Zhang, X. Gu and C. Hu, *Nano Energy* 2019, **57**, 379-387.

[S6] H. Liang, C. Xia, A.-H. Emwas, D.H. Anjum, X. Miao and H.N. Alshareef, *Nano Energy* 2018, **49**, 155-162.

[S7] K. Chi, Z. Zhang, Q. Lv, C. Xie, J. Xiao, F. Xiao and S. Wang, *ACS Appl. Mater. Interfaces* 2017, **9**, 6044-6053.

[S8] D. Chen, S. Zhou, H. Quan, R. Zou, W. Gao, X. Luo and L. Guo, Chem. Eng. J. 2018, 341, 102-111.

[S9] Z. Zhou, Q. Zhang, J. Sun, B. He, J. Guo, Q. Li, C. Li, L. Xie, Y. Yao, ACS nano 2018, 12, 9333-9341.